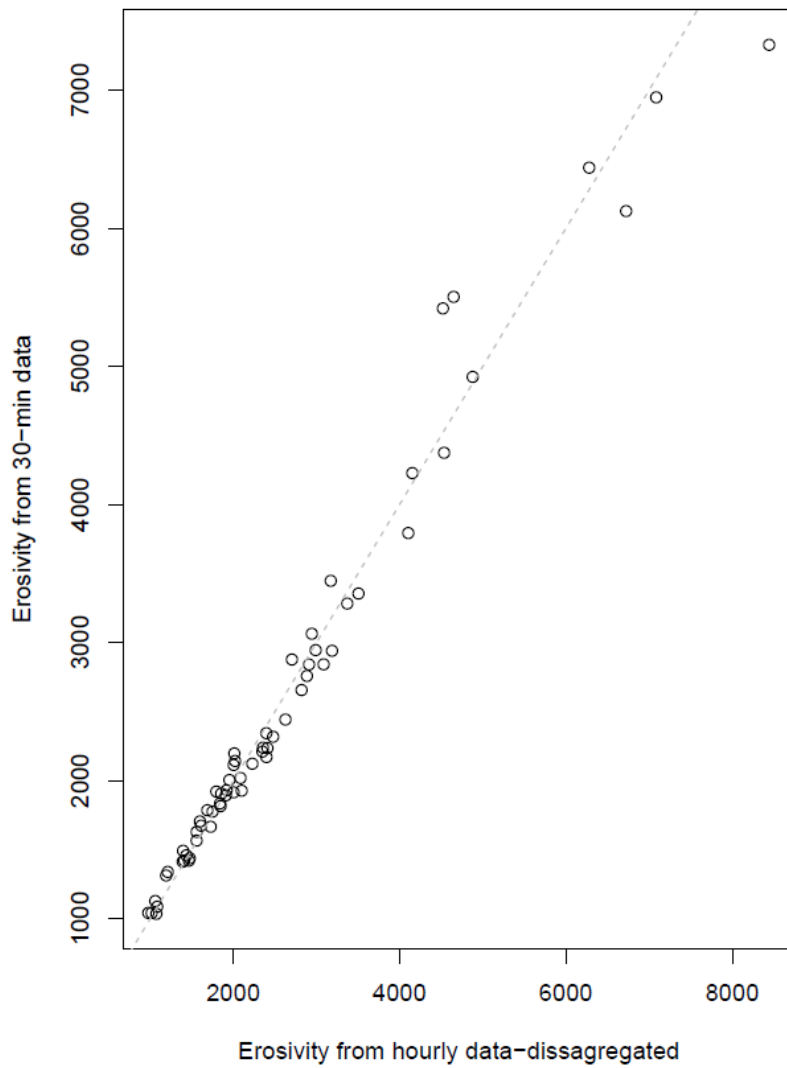
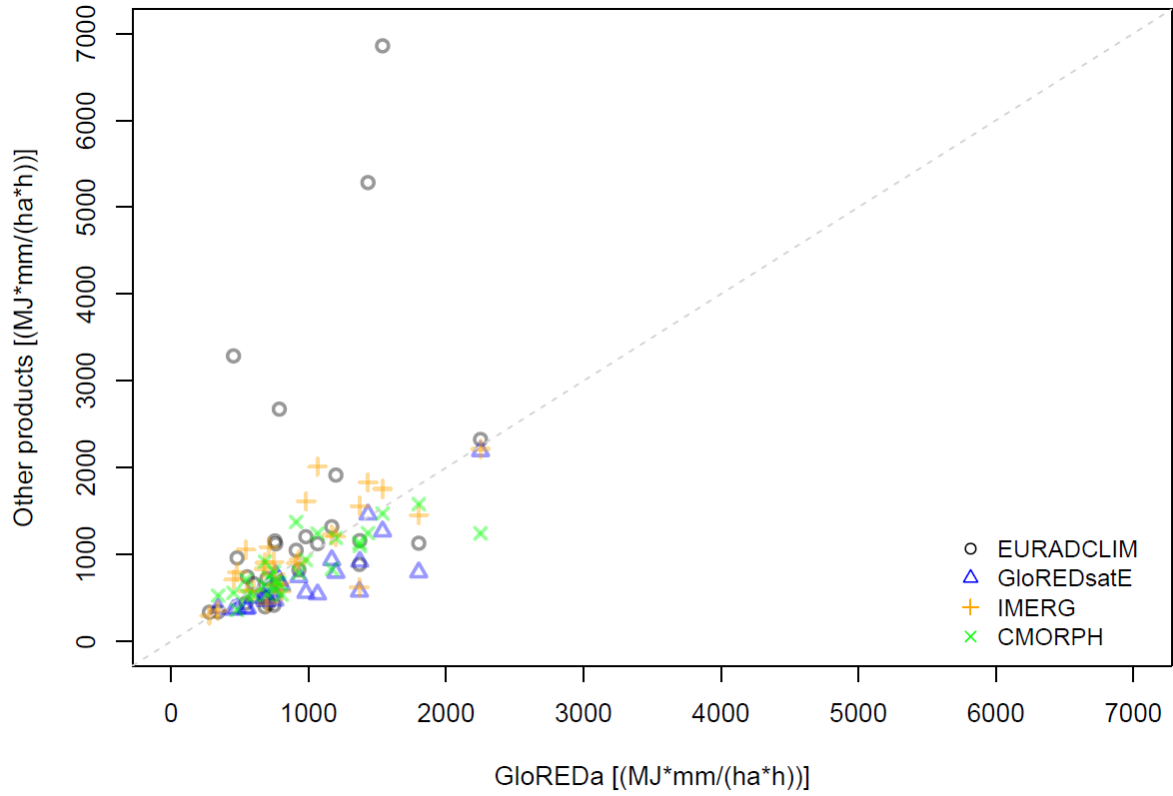


**Supplement to: Dynamic assessment of rainfall erosivity in Europe: evaluation of EURADCLIM ground-radar data**



**Figure S1: Comparison between rainfall erosivity calculated based on the 30-min rainfall data and based on the rainfall erosivity calculated based on the disaggregated rainfall data (i.e., where 25 % of rainfall was considered in first 30-min and 75 % of rainfall in second 30-min).**



**Figure S2: Comparison between annual rainfall erosivity for GloREDA (Panagos et al., 2023), EURADCLIM (this study), GloREDSatE (Das et al., 2024), IMERG (Das et al., 2024) and CMORPH (Bezák et al., 2022). Only European countries (country-average values were used) covered by EURADCLIM are shown.**

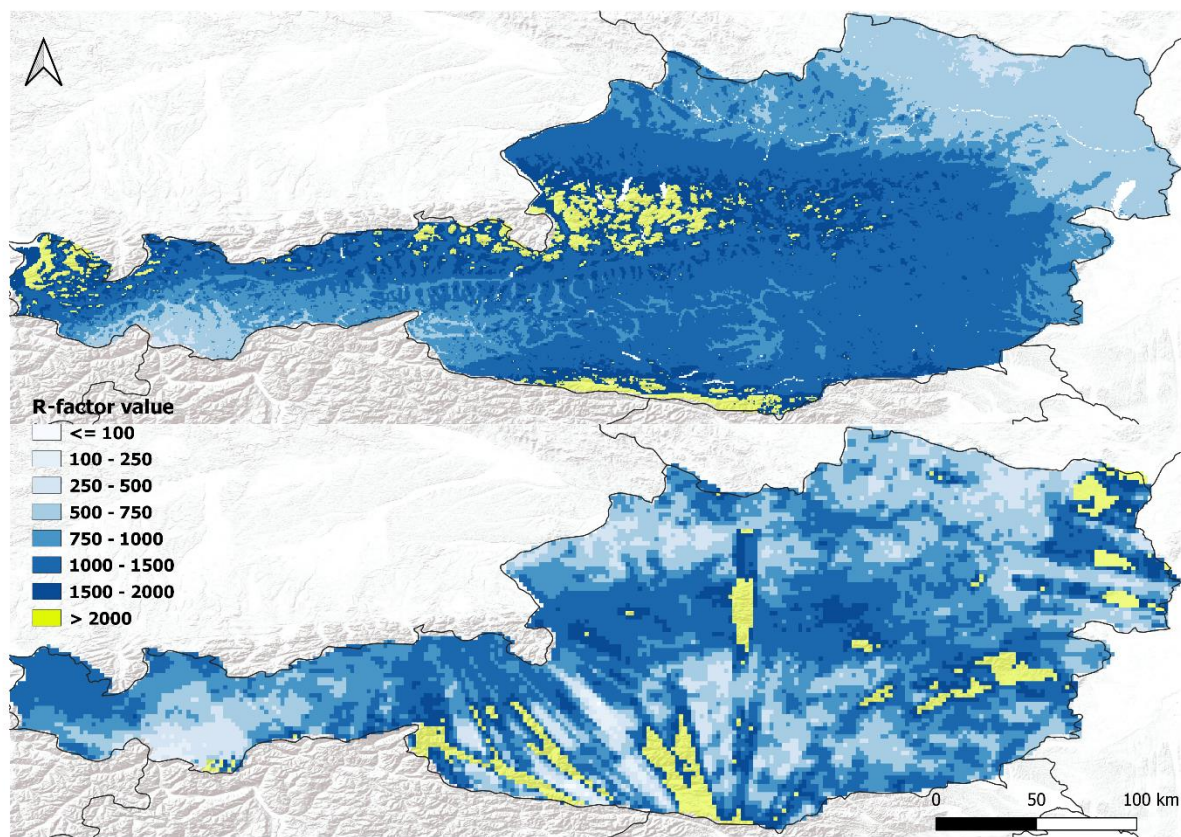


**Figure S3: Comparison between the average annual rainfall erosivity ( $\text{MJ mm ha}^{-1} \text{h}^{-1}$ ) for Austria derived based on the GloREDa (upper) and EURADCLIM (lower) predictions. Linear features represent the propagation of artefacts into the unadjusted EURADCLIM-derived rainfall erosivity.**

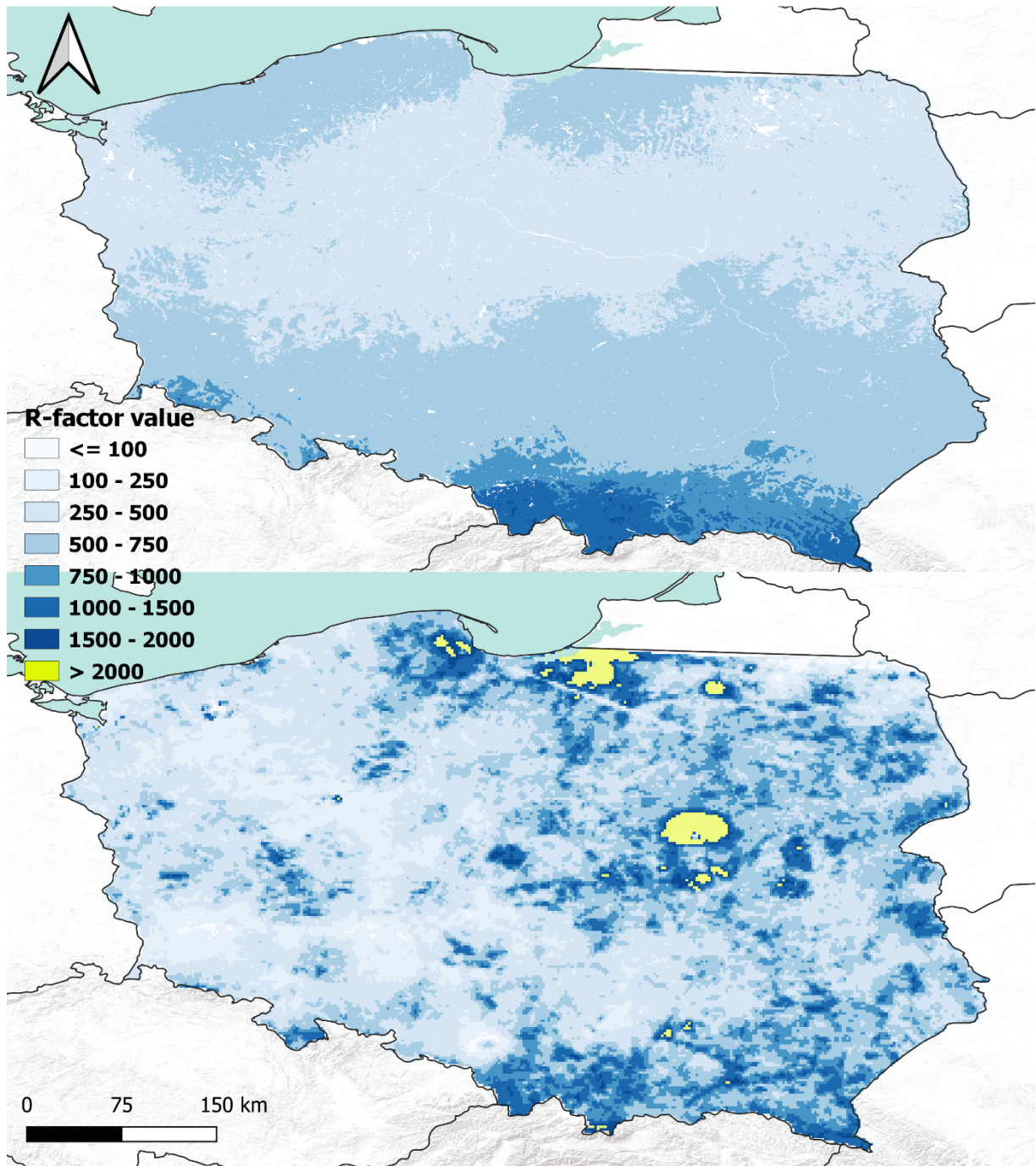
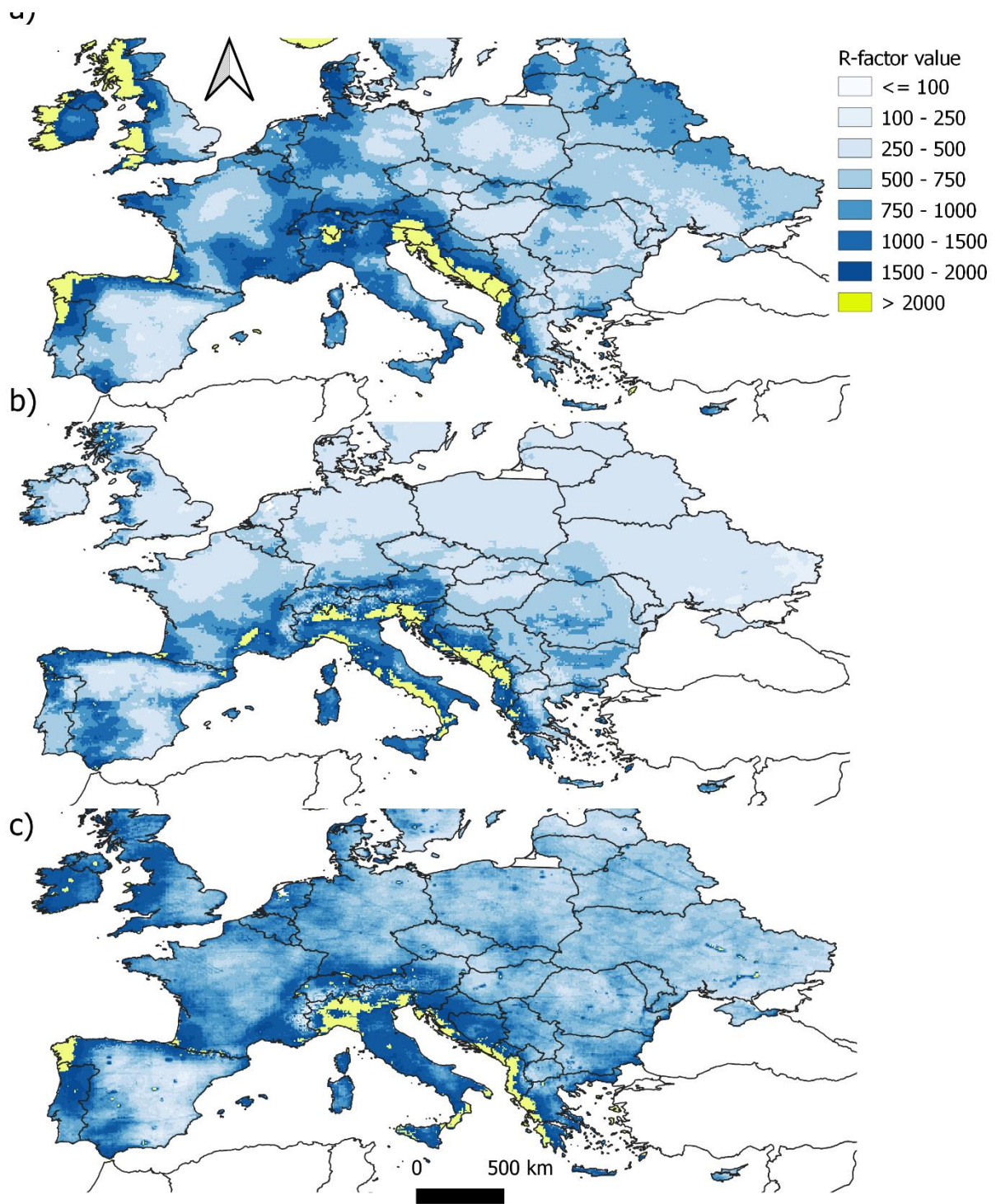
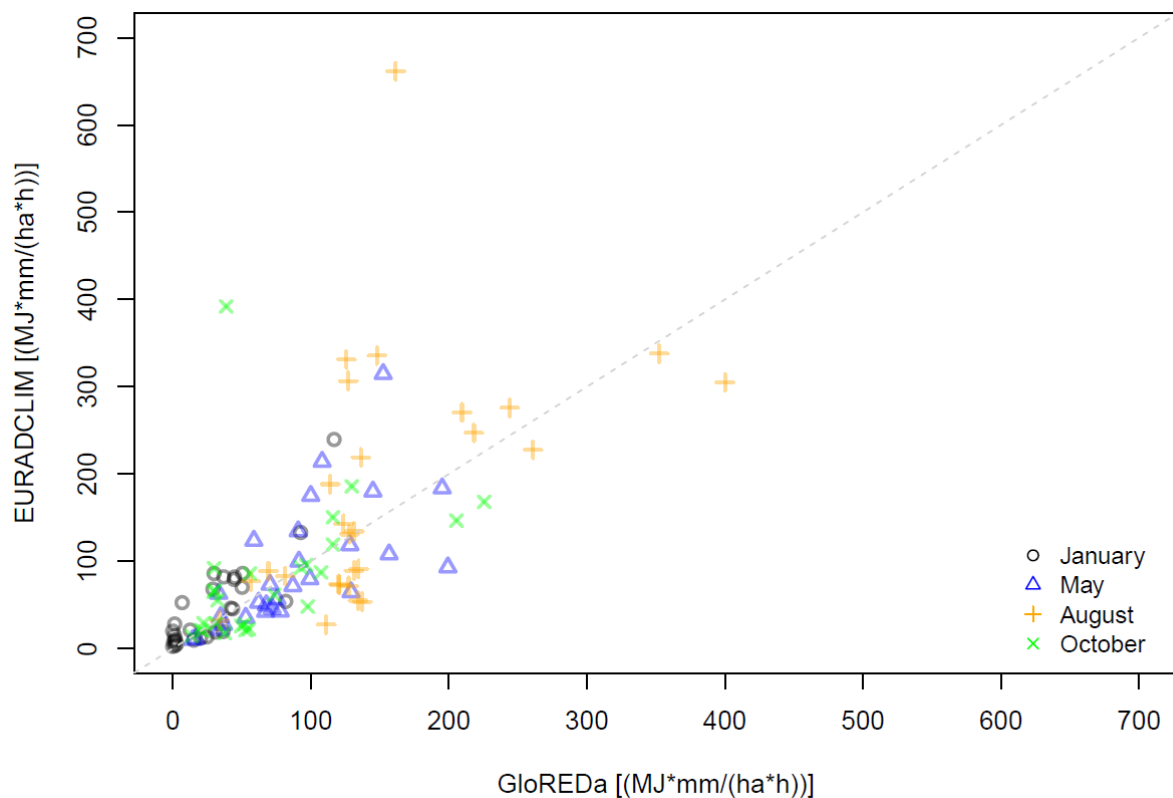


Figure S4: Comparison between annual rainfall erosivity ( $\text{MJ mm ha}^{-1} \text{h}^{-1}$ ) for Poland derived based on the EURADCLIM (upper) and GloREDa (lower) datasets.





**Figure S5:** Comparison between rainfall erosivity (R) ( $\text{MJ mm ha}^{-1} \text{h}^{-1}$ ) calculated using IMERG dataset (a), GloRESatE dataset (b) and CMORPH (c) for Europe. Maps a) and b) are adopted after Das et al. (2024). Map c) is adopted after Bezak et al. (2022).



**Figure S6: Comparison between monthly rainfall erosivity for January, May, August and October based on the EURADCLIM (x-axis) and GloREDA (y-axis) datasets.**

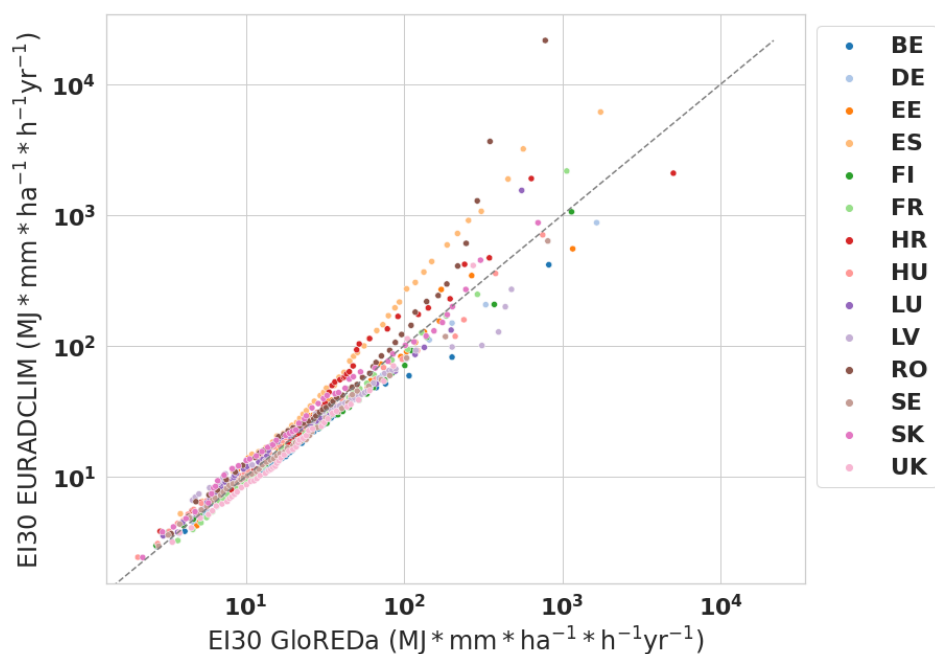


**Figure S7: Quantile-Quantile plots between GloREDA and EURADCLIM EI30 events for the year 2013. Points are coloured based on the country. It should be noted that both x and y axis are shown in log-scale.**

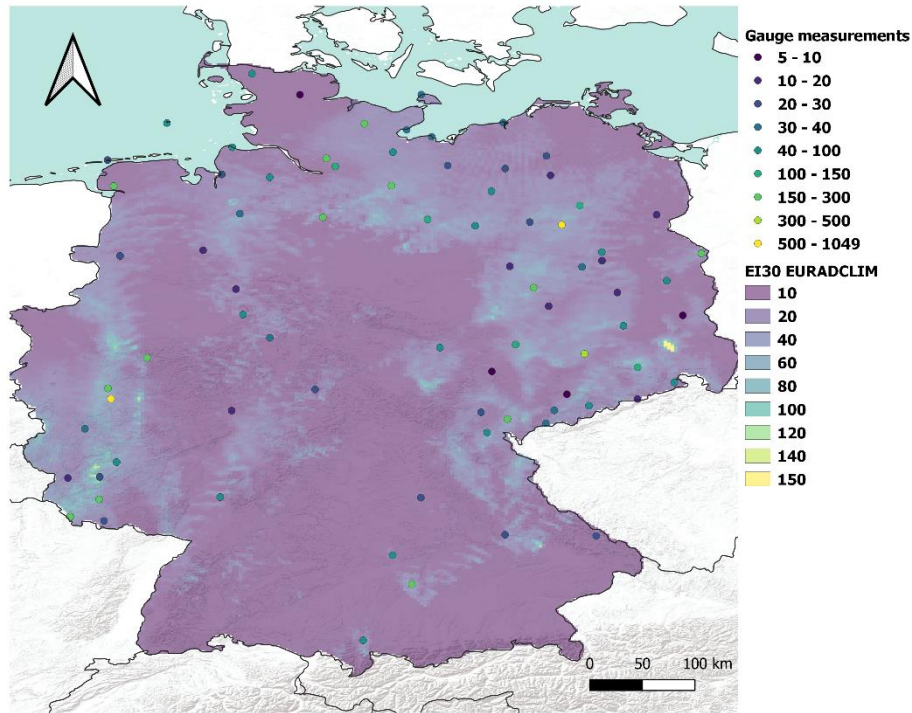


Figure S8: Comparison between spatial rainfall erosivity (EI30) patterns detected by EURADCLIM for the event that occurred on the 20<sup>th</sup> of June 2013 and the corresponding GloREDa station measurements.

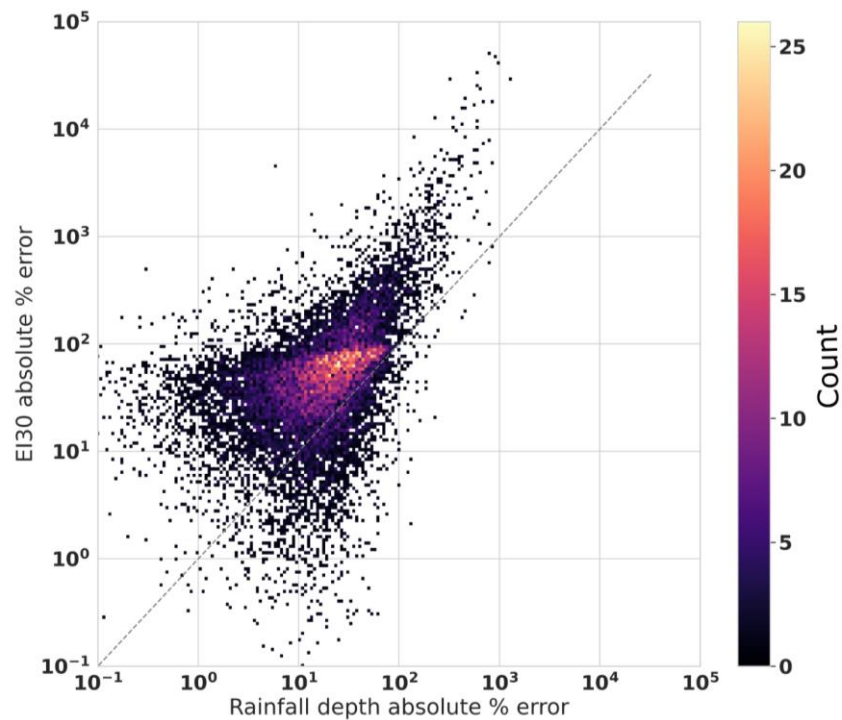
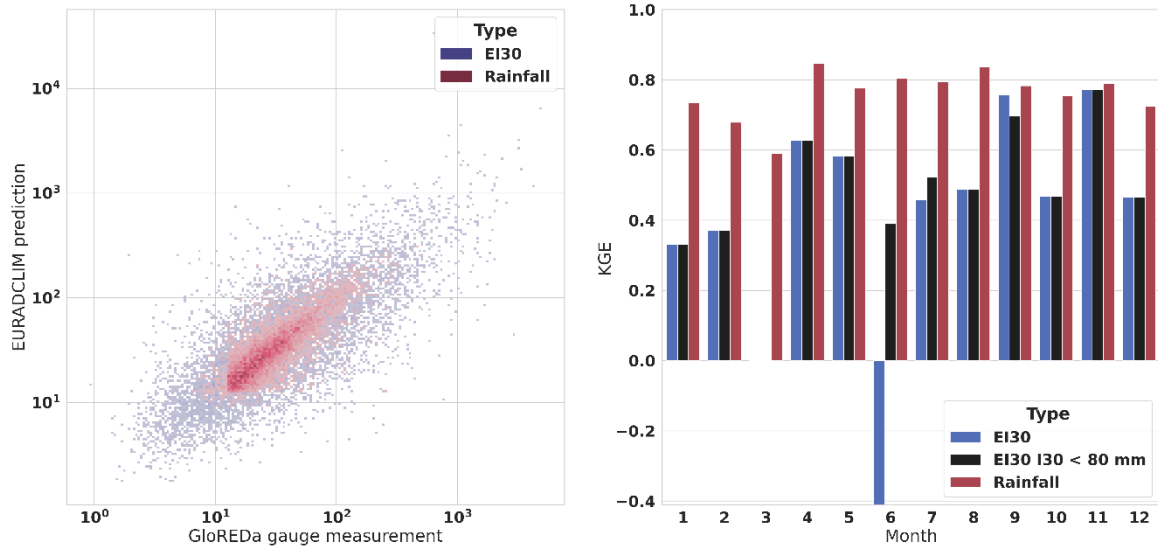
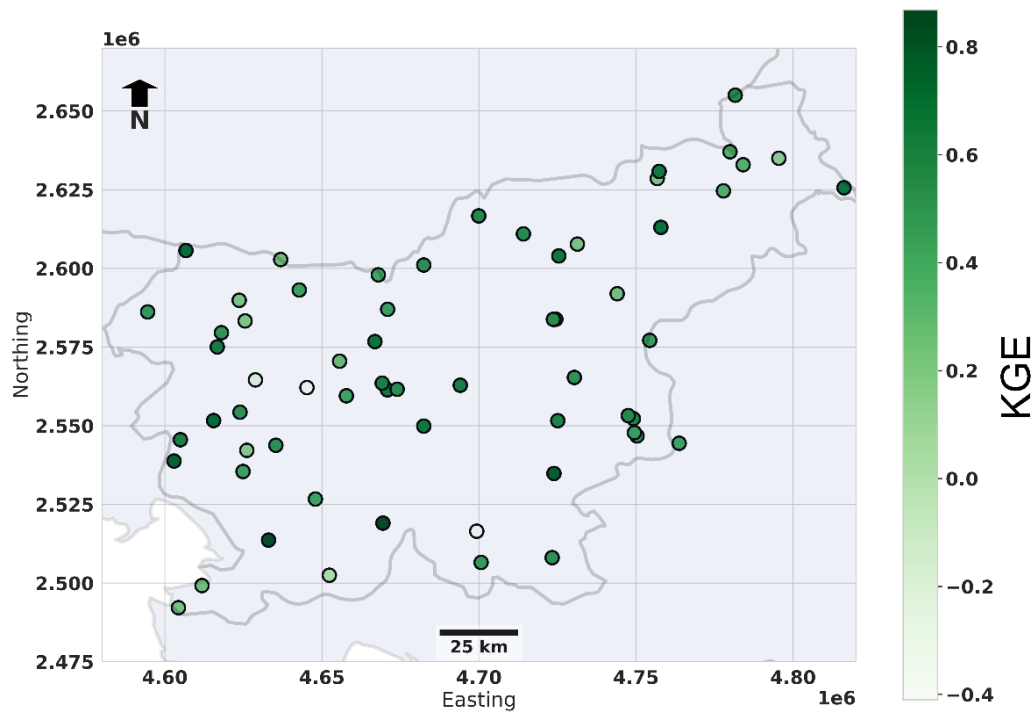


Figure S9: A comparison between the absolute % error between event rainfall depth predictions by EURADCLIM and computed EI30 value. The central dotted line depicts an equal ratio of relative error on the rainfall depth predictions to the error on the EI30.



**Figure S10: Left: Comparisons of predicted rainfall depth and EI30 from EURADCLIM against rain gauge measurements in Slovenia between 2016 and 2020. Right: Monthly evaluations of the predicted EI30 and rainfall depth via the Kling-Gupta index using an unlimited I30 (blue) and an I30 limited to 80 mm/h (black).**



**Figure S11: Location specific evaluations of EURADCLIM predictions of EI30 across Slovenia between 2016 and 2020. The KGE represents the Kling-Gupta Efficiency.**



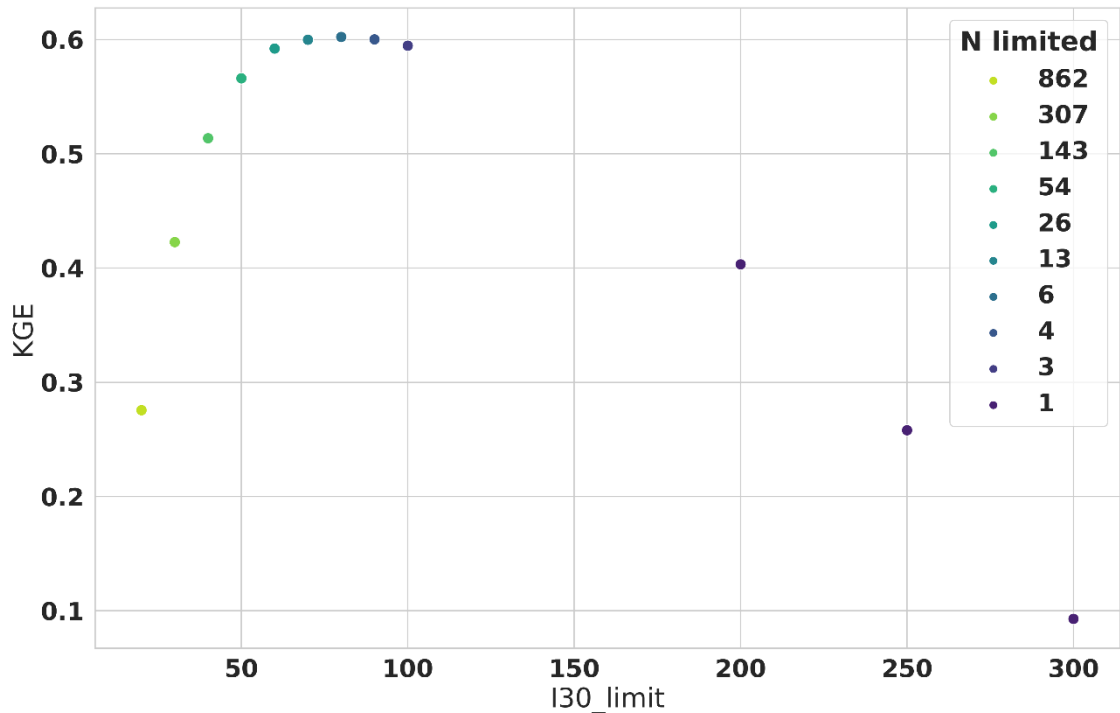


Figure S12: Comparison of impact of different I30 threshold values applied to the EURADCLIM-derived EI30 for the Slovenian stations included in the GloREDA for the 2016-2020 period. The points show the trend in the Kling-Gupta Efficiency when differing limits were applied in the calculation of EI30. "N limited" shows the number of EI30 events affected for each I30 limit, showing the changing number of impacted events when limits (less) stricter limits are applied.

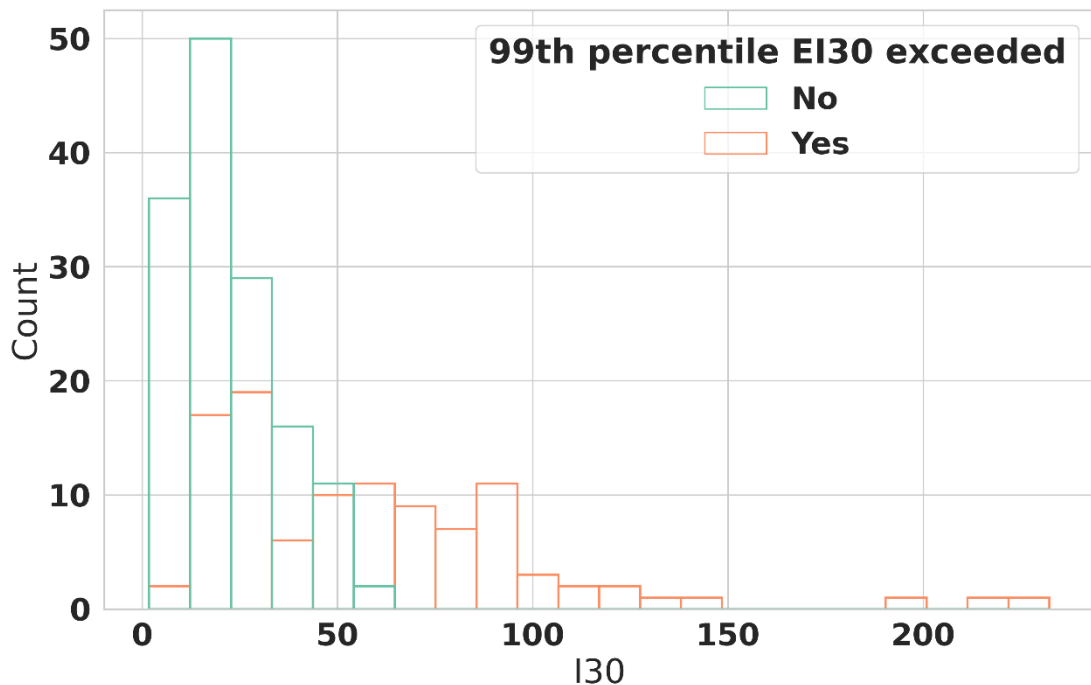


Figure S13: The populations of event-scale I30 in which the 99<sup>th</sup> percentile EI30 value was exceeded by EURADCLIM (Yes) or not (No) compared to GloREDA. Each data point is generated based on the 99<sup>th</sup> percentile EI30 value per country per month (i.e. 12 values per country). The histograms show the general separability of populations, in which overpredictions at high quantiles are characterised by unrealistic I30 values derived from EURADCLIM.